www.cadanda.com
Computer-Aided Design AND APPLICATIONS

# Development of a Meso-scale Machine Tool and the Preliminary Cutting Tests of Oxygen-free Copper Using a Polycrystalline Diamond Tool

Fang-Jung Shiou[1], Kuang-Chao Fan[2], Kai-Ming Pan[3] and Zhi-Yuan Ke[4]

[1] National Taiwan University of Science and Technology, shiou@mail.ntust.edu.tw
[2] National Taiwan University, fan@ntu.edu.tw
[3] National Taiwan University of Science and Technology, D9703206@mail.ntust.edu.tw
[4] National Taiwan University, r96522701@ntu.edu.tw

## ABSTRACT

This work presents the development of a meso-scale 3-axis milling machine with a nanometer resolution. Regarding the Z-axis design of the meso-scale 3-axis milling machine, it mainly includes a pagoda structure, the high speed air bearing spindle, two HR8 ultrasonic motors, a laser diffraction grating interferometer system (LDGI), and a coaxial counter-balance system for the spindle. The optimal geometrical dimensions of the pagoda structure have been determined by ANSYS software. According to the simulation results, the maximum static deformation along the z-axis of the pagoda was about 5.05 nm. The designed meso-scale 3-axis milling machine is equipped with an X-Y coplanar positioning stage with nanometer resolution, including the low-cost components and two ultrasonic motors, in order to reduce the complexity and error resulted from the combination of a long-stroke stage and short-travel stage. The coplanar stage developed by Nation Taiwan University was integrated with two laser diffraction grating interferometer system as displacement feedback sensors, so that a two-axis closed-loop control was possible. The positioning accuracy of the coplanar stage was about 50nm after error compensation using the gate mode, base on the test results. A circular positioning test with the radius of 7 mm using the developed stage was tested, and the overall roundness error was about 0.094 μm based on the preliminary test results. A preliminary cutting tests for the oxygen-free copper using a polycrystalline diamond tool have been investigated with respect to different depth of cut and cutting speed on the developed meso-scale machine tool.

**Keywords:** 3-axis milling machine, pagoda structure, polycrystalline diamond tool.
**DOI:** 10.3722/cadaps.2012.631-640

## 1 INTRODUCTION

The demands in the micro-mechanical have been increased such as digital cameras, mobile phones, sensors, actuators and so on in the past decade [1]. The precision manufacturing process would be able to manufacture microstructures with 3D complex shapes or free-form surfaces [2]. Therefore, there are more and more researches focus on high precision machine tool design and manufacturing such as precision turning machine [3], precision grinding machine [4] and micro-milling machine [5].

Designing a precision machine, four major subsystems have to be taken into account, including mechanical structure, drive, spindle and control system. The precision machine mechanical structure design and analysis have been discussed in [6].

Regarding diamond tool machining, J.H. Lee et al.[7] used diamond tool to fabricate v-groove on the optical fiber connector. Jiwang Yan et al. [8] used single crystal diamond tool for machining v-groove on an electroless-plated Nip surface and used as molds for hot-press glass. Gi Dae Kim et al. [9] discussed the new method using single crystal diamond tool to manufacture v-groove machining, in which an ultrasonic elliptical vibration method was applied to reduce the burrs formation and reduce the cutting force.

The price of an ultra-precision manufacturing machine generally more than NTD 10 million, and most of them are export-restricted products. For that reason, the objective of this research is to develop an economy meso-scale 3-axis milling machine with a nanometer resolution that can be applied to do shaping and high speed milling machining.

## 2 DESIGN AND ANALYSIS OF THE MESO-SCALE 3-AXIS MILLING MACHINE TOOL

The purpose of this study is to develop a meso-scale 3-axis machine tool with nanometer resolution. The schematic illustration of the meso-scale 3-axis machine tool, the Z-axis design and its static deformation analysis, the design of high speed air baring spindle clamp and driving mechanism, the design of the XY-coplanar stage, the system integration and some test results of the assembled machine tool were introduced in the next sections.

### 2.1 Design of the meso-scale 3-axis machine tool

The conceptual design of a high-precision micro-milling machine tool, including a pagoda structure, the high speed air bearing spindle, two HR8 ultrasonic motors, three laser diffraction grating interferometer systems (LDGI), a micro dynamometer, a coaxial counter-balance system, XY coplanar positioning stage, CNC controller and an industrial PC, is shown in Fig. 1. Table 1 shows the specification of the designed high-precision micro-milling machine tool.

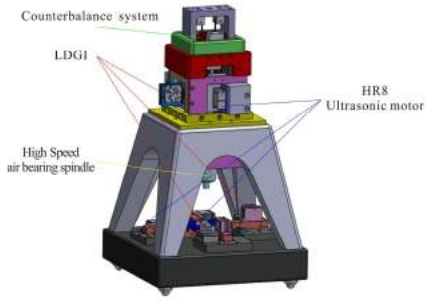


Fig. 1: Schematic of the meso-scale 3-axis milling machine tool and its control system.

| | |
|---|---|
| *Machine size (LWH)* | 500 mm × 500 mm × 600 mm |
| *Working Range (XYZ)* | 25 mm × 25 mm × 10 mm |
| *Driven system* | Ultrasonic motor |
| *Speed range* | 80,000 rpm (Max) |
| *Resolution* | ±50 nm |

Tab. 1: Machine specification.

## 2.2 Z-axis design and analysis

### *2.2.1 Optimal geometrical dimensions of the pagoda structure design*

The design of the structure of meso-scale machine tool must take into account the rigidity to withstand the weight of the spindle system. As a result, according to the former design of several different shapes of the machine tool structure, and using ANSYS finite element analysis software to analyze the best machine structure, the result of the pagoda-type structure was the most stable [10]. This work follows previous pagoda-type structure design, and makes some improvements design to clamp and integrate the new Z-axis for a high speed air bearing spindle. The optimal geometrical dimensions of the pagoda structure have been determined by ANSYS software. Figure 2 shows the new design of Z-axis of the granite pagoda. The optimal geometrical dimensions of the newly designed pagoda structure parameters are listed in Table 2.

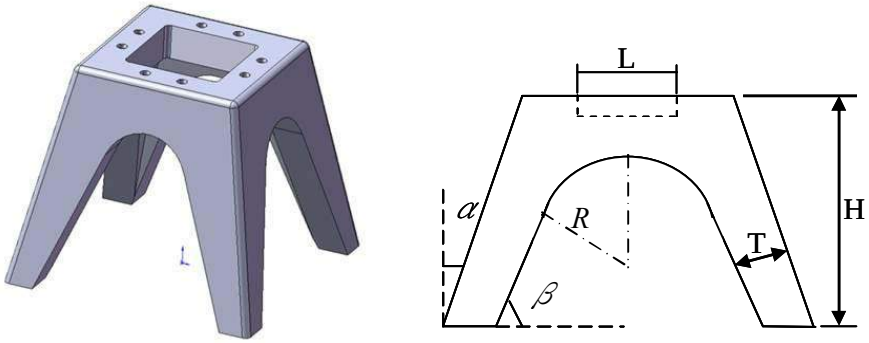


Fig. 2: Pagoda and its key parameters.

| Each Part | Size |
|---|---|
| R | 90 mm |
| □ | 78 |
| T | 50 |
| H | 430 mm |
| L | 130 mm |

Tab. 2: Optimal geometrical dimensions of the pagoda structure.

### *2.2.2 The high speed air bearing spindle clamp and driven mechanism in Z-axis*

There are four main parts in the design of high speed air baring spindle clamp and driving mechanism, including the counterbalance system, LDGI, ultrasonic motor, and high speed air bearing spindle system, as shown in Fig. 4. High speed air bearing spindle clamp and driver consists of two ultrasonic motors to drive the spindle clamp with seesaw motion. Furthermore, a set of LDGI is used as displacement feedback sensor with nanometer resolution to measure the displacement of Z-axis, to execute close loop control.

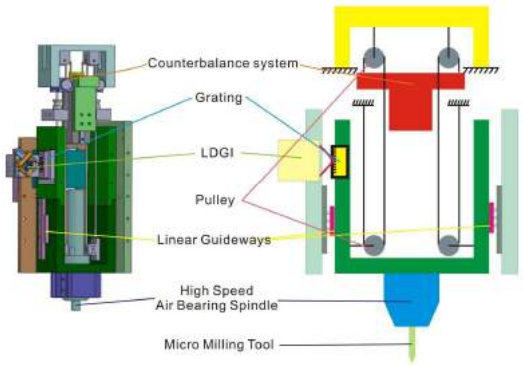


Fig. 4: The high speed air bearing spindle clamp and driven mechanism in Z-axis.

### *2.2.3 Z-axis mainly parts and preliminary assembly*

This study completed the Z-axis design and manufacturing, and assembly, including a pagoda structure, the high speed air bearing spindle clamp, two HR8 ultrasonic motors, a laser diffraction grating interferometer system (LDGI) [11], and a coaxial counter-balance system for the spindle. The assembled three-axis micro-milling machine tool is shown in Fig.5.

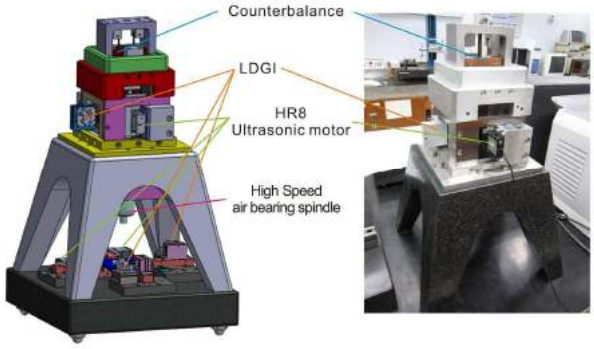


Fig. 5: Assembled meso-scale 3-axis milling machine tool.

## 2.3 XY coplanar positioning stage design and analysis

### *2.3.1 XY coplanar positioning stage design*

The coplanar stage developed by Nation Taiwan University was integrated with two laser diffraction grating interferometer systems as the displacement feedback sensors. Two HR8 ultrasonic motors are used as driving motors, and 8 linear guides are used to perform the coplanar movement without Abbeís error [12]. The design of the XY-coplanar stage is shown in Fig. 6, and the assembled coplanar stage is shown in Fig. 7.

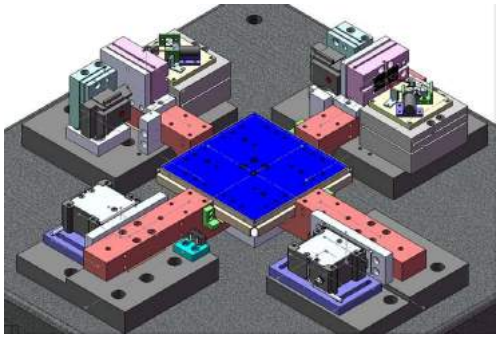

Fig. 6: The schematic of XY-coplanar stage.

Fig. 7: Photo of the XY-coplanar stage.

### *2.3.2 XY coplanar positioning stage tilting angle of stage at different positions*

After assembly the laser interferometer (SIOS MI-5000) was used to measure the X- and Y-axis tilting angles. Figure 8 shows the measured results of pitch angles. The maximum tilting angles for X- and Y-axis within the travel of 22 mm, were about 5 and 4 arc-seconds, respectively. The open loop positioning error for X- and Y-axis within the travel of 20 mm was about 0.205 μm, as shown in Fig. 9.

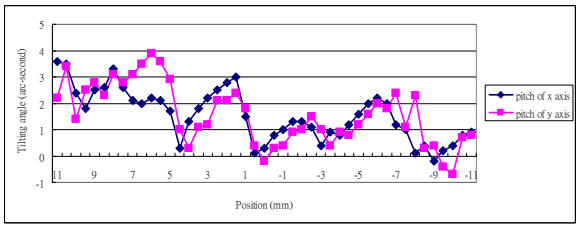


Fig. 8: X and Y pitch angle of stage at different positions.

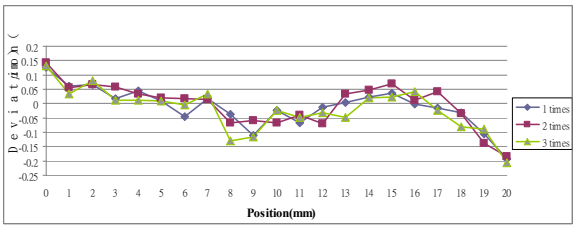


Fig. 9: The XY-coplanar stage positioning error.

## 2.4 System integration and test results

To implement the closed loop control the XY-coplanar stage, a NI DAQ 6259 was adopted in this research. The XY stage control flow chart for the coplanar stage is shown in Fig. 10 [13]. The X-, and Y-axis of the coplanar stage were driven by ultrasonic motors, and through DAQ device to capture the signal of FPGA connected to the feedback signals of LDGI, and transform its data to the displacement of the stage.

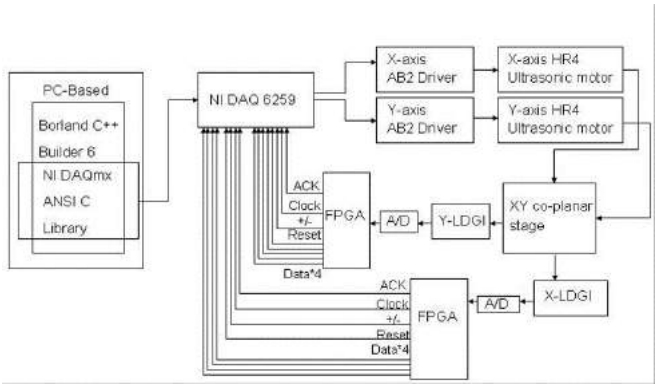


Fig. 10: The XY stage control flow chart.

The closed loop positioning errors of the X- and Y-axis, were about ± 0.1 μm within the travel of 11 mm, as shown in Fig. 11 and Fig. 12, respectively, according to the test results.

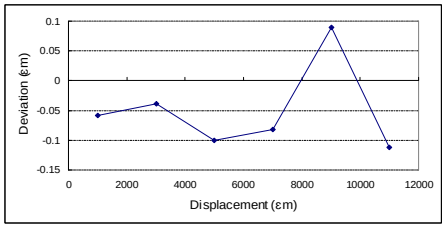


Fig. 11: X-axis positioning accuracy.

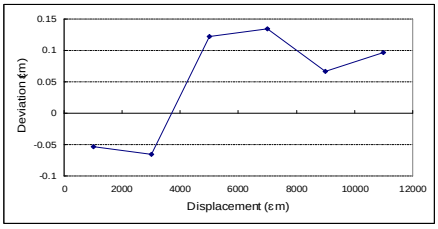


Fig. 12: Y-axis positioning accuracy.

A preliminary circular test with the radius of 7 mm has also been carried out in this study. The roundness error of the circular positioning test is about 0.094 μm, as shown in Fig 13.

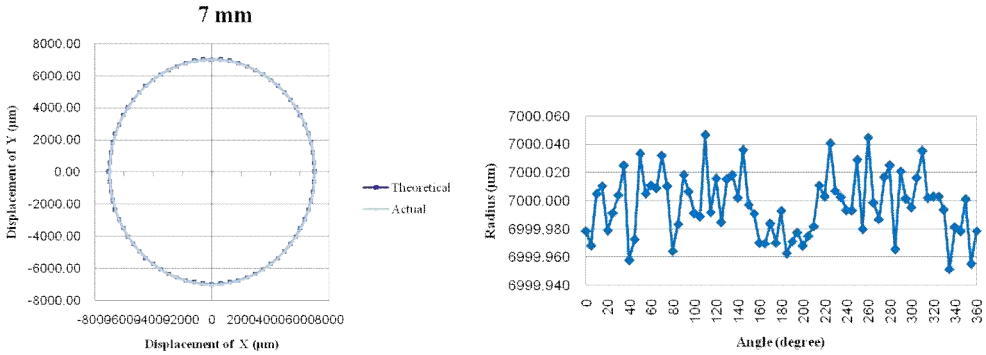


Fig. 13: Circular positioning test with the radius 7 mm.

## 3 PRELIMINARY CUTTING TEST USING A POLYCRYSTALLINE DIAMOND TOOL

In this study, the experiment conducted a preliminary research for machining micro V-grooves of oxygen-free copper using a polycrystalline diamond tool on the developed meso-scale 3-axis milling machine tool. The schematic of the meso-scale 3-axis milling machine tool is shown in Fig. 14. Figure 15 shows the photo of the cutting test using a polycrystalline diamond tool. Three shaping parameters, namely depth of cut, pitch, feed rate, were investigated in this study. The configured path for the experiments was driven by an industrial computer controller (ELC2200) to drive ultrasonic motors of the XY co-planar stage. After conducting the micro machining experiments, the structures of grooves were observed by an optical microscope.

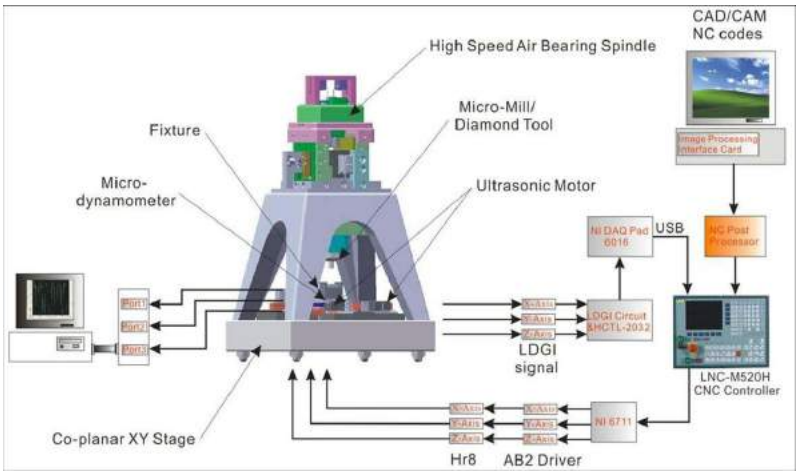


Fig. 14: Schematic of the Meso-scale 3-axis milling machine tool and control system.

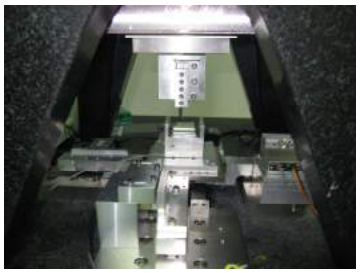

Fig. 15: Photo of the cutting test.

Figure 16 shows the designed drawing of a polycrystalline diamond tool made by Lu Sung Diamond Industrial Co. Ltd. in Taiwan. The fabricated tool observed by a toolmaker microscope is shown in Fig. 17.

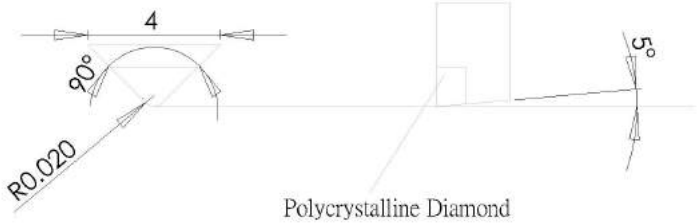


Fig. 16: The designed drawing of the polycrystalline diamond tool.

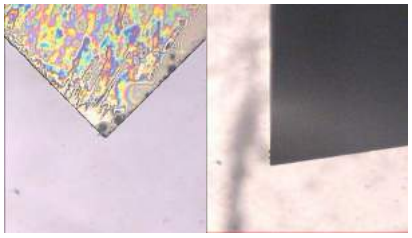

Fig. 17: Photo of polycrystalline diamond tool (30X).

The oxygen-free high conductivity copper (OFHC) was used for the study. Before executing the V groove shaping, the work-piece was ground and polished to increase the flatness and surface roughness. The mean polished surface roughness of the specimen was Ra 0.03 μm.

The selected primary cutting parameters for shaping process are feed rate and depth of cut. The feed rate is configured as 1.5, 2.0 and 2.5 mm/s, respectively. The depth of cut is configured as 5, 10 and 15 μm, respectively. The shaping travel was 5.0 mm. The induced cutting forces were measured by a micro dynamometer. After finishing experiments, the optical microscope was used to inspect the wear and surface of the diamond tool.

This study has accomplished various combinational experiments of the depth of cut and feed rate, namely 1.5, 2.0, 2.5mm/s and 5, 10, 15 μm. The top view as shown in Fig. 19. The induced force under various feed rate measured by a micro dynamometer were shown in figure 20~22. The measured cutting force for the feed rate of 1.5, 2.0, 2.5mm/s were about 0.50N, 0.55N and 0.60 N, respectively. In addition, the positioning error of the V-grooves with 100 $\mu$m pitch was also investigated, as shown in Fig. 23. The results showed the average pitch of the V-grooves was 100.967 μm.

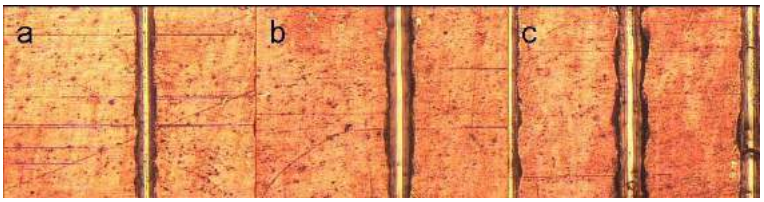


Fig. 19: The top view for different depth of cut (a) 5 μm depth of cut; (b) 10 μm depth of cut and (c) 15 μm depth of cut (100X).

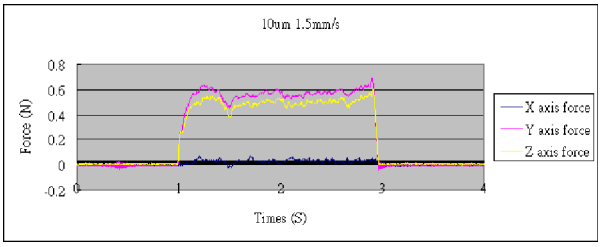


Fig. 20: The cutting force by depth of cut 10 μm and cutting speed 1.5 mm/s.

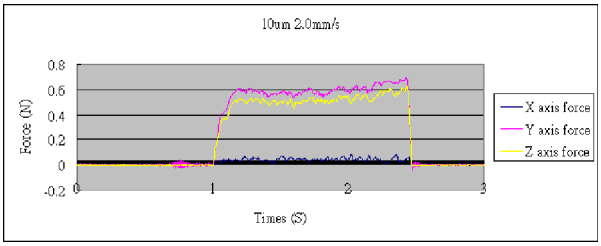


Fig. 21: The cutting force by depth of cut 10 μm and cutting speed 2.0 mm/s.

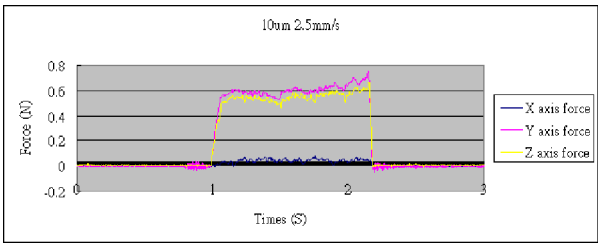


Fig. 22: The cutting force by depth of cut 10 μm and cutting speed 2.5 mm/s.

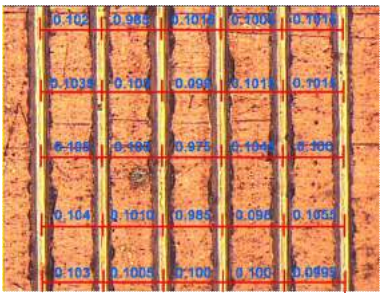

Fig. 23: Photo of the V-grooves with a pitch of 100 μm.

## 4 CONCLUSION

A prototype of the meso-scale 3-axis milling machine tool with a nanometer resolution has been newly developed in this work. Some preliminary test results of the coplanar stage have been carried out in this work. The maximum tilting angles of the new coplanar stage for X- and Y-axis within the travel of 22 mm, were about 5 and 4 arc-seconds, respectively. The open loop positioning error for X- and Y-axis within the travel of 20 mm was about 0.205 μm. The closed loop positioning errors of the X- and Y-axis, were about 0.1 m within the travel of 11 mm. The roundness error of the preliminary circular positioning test was about 0.094 mm. A preliminary cutting tests for the oxygen-free copper using a polycrystalline diamond tool have been executed with respect to different depth of cut and cutting speed on the developed meso-scale machine tool. The induced cutting force measured by the micro dynamometer has also been investigated. The accuracy of the developed machine tool will be further improved in the future using an appropriate control strategy.

## 5 ACKNOWLEDGEMENTS

The authors are grateful to the Nation Science Council of the Republic of China for supporting this research under grant NSC 98-2221-E-011-100MY2.

## 6 REFERENCES

[1] Dornfeld, D.; Min, S.; Takeuchi, Y.: Recent advances in mechanical micromachining, CIRP Annals - Manufacturing Technology, 55(2), 2006, 745-768

[2] http://www.cpzl.com/news/articleview/2006-7-14/ar

[3] http://www.nanotechsys.com/index.html

[4] http://www.loadpoint.co.uk/products/machinery/picoace.html

[5] http://www.fanuc.co.jp/eindex.htm

[6] Luo, X.; Cheng, K.; Webb, D.; Wardle, F.: Design of ultra-precision machine tools with applications to manufacture of miniature and micro components, Journal of Materials Processing Technology, 167(2-3), 2005, 515-528.

[7] Lee, J.H.; Park, S.R.; Yang, S.H.; Kim, Y.S.: Fabrication of a V-groove on the optical fiber connector using a miniaturized machine tool, Journal of Materials Processing Technology, 155-156(1-3), 2004, 1716-1722. doi: 10.1016/j.jmatprotec.2004.04.152

[8] Yan, J.; Oowada, T.; Zhou, T.; Kuriyagawa, T.: Precision machining of microstructures on electroless-plated NiP surface for molding glass components, Journal of Materials Processing Technology, 209(10), 2009, 4802-4808. doi: 10.1016/j.jmatprotec.2008.12.008

[9] Kim, G.D.; Loh, B.G.: An ultrasonic elliptical vibration cutting device for micro V-groove machining: Kinematical analysis and micro V-groove machining characteristics, Journal of Materials Processing Technology, 190(1-3), 2007, 181-188. doi:10.1016/j.jmatprotec.2007.02.047

[10] Fan, K.-C.; Fei, Y.; Yu, X.; Wang, W.; Chen, Y.: Study of a noncontact type micro-CMM with arch-bridge and nano-positioning stages, Robotics and Computer-Integrated Manufacturing, 23(3), 2007, 276-284. doi: 10.1016/j.rcim.2006.02.007

[11] Fan, K.-C.; Li, B.-K.; Liu, C.-H.: A diffraction grating scale for long range and nanometer resolution, Proceedings of SPIE - The International Society for Optical Engineering, 7133, 2009, art. no. 71334J. doi: 10.1117/12.815188

[12] Abbe, C.: Popular errors in meteorology, Journal of the Franklin Institute, 123(2), 1887, 115-128.

[13] Cheng, F.; Fan, K.-C.; Fei, Y.-T.: A robust control scheme of nanopositioning driven by ultrasonic motor, Proceedings of SPIE - The International Society for Optical Engineering, 7130, 2008, art. no. 71301O. doi: 10.1117/12.819598